EUROPEAN ORGANIZATION FOR NUCLEAR RESEARCH

CERN–PPE/94–132

5 August 1994

Measurement of time dependent $B^0_d - \bar{B}^0_d$ mixing

DELPHI Collaboration

Abstract

The time dependent mixing of $B^0_d - \bar{B}^0_d$ mesons has been observed by using the correlations between the charge of D^* mesons and the weighted mean charge of particles in each hemisphere.
From a reconstructed $D^{*\pm}$ sample corresponding to about 1.7 million hadronic Z^0 decays, the mass difference between the two B^0_d mass eigenstates has been measured to be

$$\Delta m = 0.50 \pm 0.12(stat) \pm 0.06(syst)\ \hbar/ps$$

or, converting into eV/c^2:

$$\Delta m = [3.29 \pm 0.79(stat) \pm 0.39(syst)]\ \ 10^{-4}\ eV/c^2.$$

(To be submitted to Physics Letters B)

P.Abreu[20], W.Adam[7], T.Adye[37], E.Agasi[30], I.Ajinenko[42], R.Aleksan[39], G.D.Alekseev[14], P.P.Allport[21], S.Almehed[23], F.M.L.Almeida[47], S.J.Alvsvaag[4], U.Amaldi[7], A.Andreazza[27], P.Antilogus[24], W-D.Apel[15], R.J.Apsimon[37], Y.Arnoud[39], B.Åsman[44], J-E.Augustin[18], A.Augustinus[30], P.Baillon[7], P.Bambade[18], F.Barao[20], R.Barate[12], D.Y.Bardin[14], G.J.Barker[34], A.Baroncelli[40], O.Barring[7], J.A.Barrio[25], W.Bartl[50], M.J.Bates[37], M.Battaglia[13], M.Baubillier[22], J.Baudot[39], K-H.Becks[52], M.Begalli[36], P.Beilliere[6], K.Belous[42], P.Beltran[9], A.C.Benvenuti[5], M.Berggren[41], D.Bertrand[2], F.Bianchi[45], M.Bigi[45], M.S.Bilenky[14], P.Billoir[22], J.Bjarne[23], D.Bloch[8], J.Blocki[51], S.Blyth[34], V.Bocci[38], P.N.Bogolubov[14], T.Bolognese[39], M.Bonesini[27], W.Bonivento[27], P.S.L.Booth[21], G.Borisov[42], C.Bosio[40], B.Bostjancic[43], S.Bosworth[34], O.Botner[48], B.Bouquet[18], C.Bourdarios[18], T.J.V.Bowcock[21], M.Bozzo[11], S.Braibant[2], P.Branchini[40], K.D.Brand[35], R.A.Brenner[13], H.Briand[22], C.Bricman[2], L.Brillault[22], R.C.A.Brown[7], P.Bruckman[16], J-M.Brunet[6], L.Bugge[32], T.Buran[32], A.Buys[7], J.A.M.A.Buytaert[7], M.Caccia[27], M.Calvi[27], A.J.Camacho Rozas[41], R.Campion[21], T.Camporesi[7], V.Canale[38], K.Cankocak[44], F.Cao[2], F.Carena[7], P.Carrilho[47], L.Carroll[21], R.Cases[49], C.Caso[11], M.V.Castillo Gimenez[49], A.Cattai[7], F.R.Cavallo[5], L.Cerrito[38], V.Chabaud[7], A.Chan[1], Ph.Charpentier[7], L.Chaussard[24], J.Chauveau[22], P.Checchia[35], G.A.Chelkov[14], P.Chliapnikov[42], V.Chorowicz[22], J.T.M.Chrin[49], V.Cindro[43], P.Collins[34], J.L.Contreras[18], R.Contri[11], E.Cortina[49], G.Cosme[18], F.Cossutti[46], F.Couchot[18], H.B.Crawley[1], D.Crennell[37], G.Crosetti[11], J.Cuevas Maestro[33], S.Czellar[13], E.Dahl-Jensen[28], J.Dahm[52], B.Dalmagne[18], M.Dam[32], G.Damgaard[28], E.Daubie[2], A.Daum[15], P.D.Dauncey[37], M.Davenport[7], J.Davies[21], W.Da Silva[22], C.Defoix[6], G.Della Ricca[46], P.Delpierre[26], N.Demaria[34], A.De Angelis[7], H.De Boeck[2], W.De Boer[15], S.De Brabandere[2], C.De Clercq[2], M.D.M.De Fez Laso[49], C.De La Vaissiere[22], B.De Lotto[46], A.De Min[27], L.De Paula[47], C.De Saint-Jean[39], H.Dijkstra[7], L.Di Ciaccio[38], F.Djama[8], J.Dolbeau[6], M.Donszelmann[7], K.Doroba[51], M.Dracos[8], J.Drees[52], M.Dris[31], Y.Dufour[7], F.Dupont[12], D.Edsall[1], R.Ehret[15], T.Ekelof[48], G.Ekspong[44], M.Elsing[52], J-P.Engel[8], N.Ershaidat[22], M.Espirito Santo[20], D.Fassouliotis[31], M.Feindt[7], A.Ferrer[49], T.A.Filippas[31], A.Firestone[1], H.Foeth[7], E.Fokitis[31], F.Fontanelli[11], F.Formenti[7], J-L.Fousset[26], B.Franek[37], P.Frenkiel[6], D.C.Fries[15], A.G.Frodesen[4], R.Fruhwirth[50], F.Fulda-Quenzer[18], H.Furstenau[7], J.Fuster[7], D.Gamba[45], M.Gandelman[17], C.Garcia[49], J.Garcia[41], C.Gaspar[7], U.Gasparini[35], Ph.Gavillet[7], E.N.Gazis[31], D.Gele[8], J-P.Gerber[8], P.Giacomelli[7], D.Gillespie[7], R.Gokieli[51], B.Golob[43], V.M.Golovatyuk[14], J.J.Gomez Y Cadenas[7], G.Gopal[37], L.Gorn[1], M.Gorski[51], V.Gracco[11], F.Grard[2], E.Graziani[40], G.Grosdidier[18], P.Gunnarsson[44], J.Guy[37], U.Haedinger[15], F.Hahn[52], M.Hahn[44], S.Hahn[52], S.Haider[30], Z.Hajduk[16], A.Hakansson[23], A.Hallgren[48], K.Hamacher[52], W.Hao[30], F.J.Harris[34], V.Hedberg[23], R.Henriques[20], J.J.Hernandez[49], J.A.Hernando[49], P.Herquet[2], H.Herr[7], T.L.Hessing[21], E.Higon[49], H.J.Hilke[7], T.S.Hill[1], S-O.Holmgren[44], P.J.Holt[34], D.Holthuizen[30], P.F.Honore[6], M.Houlden[21], J.Hrubec[50], K.Huet[2], K.Hultqvist[44], P.Ioannou[3], P-S.Iversen[4], J.N.Jackson[21], R.Jacobsson[44], P.Jalocha[16], G.Jarlskog[23], P.Jarry[39], B.Jean-Marie[18], E.K.Johansson[44], M.Jonker[7], L.Jonsson[23], P.Juillot[8], M.Kaiser[15], G.Kalmus[37], F.Kapusta[22], M.Karlsson[44], E.Karvelas[9], A.Katargin[42], S.Katsanevas[3], E.C.Katsoufis[31], R.Keranen[7], B.A.Khomenko[14], N.N.Khovanski[14], B.King[21], N.J.Kjaer[28], H.Klein[7], A.Klovning[4], P.Kluit[30], A.Koch-Mehrin[52], J.H.Koehne[15], B.Koene[30], P.Kokkinias[9], M.Koratzinos[32], A.V.Korytov[14], V.Kostioukhine[42], C.Kourkoumelis[3], O.Kouznetsov[14], P.H.Kramer[52], M.Krammer[50], C.Kreuter[15], J.Krolikowski[51], I.Kronkvist[23], W.Krupinski[16], W.Kucewicz[16], K.Kulka[48], K.Kurvinen[13], C.Lacasta[49], I.Laktineh[24], C.Lambropoulos[9], J.W.Lamsa[1], L.Lanceri[46], P.Langefeld[52], V.Lapin[42], I.Last[21], J-P.Laugier[39], R.Lauhakangas[13], G.Leder[50], F.Ledroit[12], R.Leitner[29], Y.Lemoigne[39], J.Lemonne[2], G.Lenzen[52], V.Lepeltier[18], T.Lesiak[35], J.M.Levy[8], E.Lieb[52], D.Liko[50], R.Lindner[52], A.Lipniacka[18], I.Lippi[35], B.Loerstad[23], M.Lokajicek[10], J.G.Loken[34], A.Lopez-Fernandez[7], M.A.Lopez Aguera[41], M.Los[30], D.Loukas[9], J.J.Lozano[49], P.Lutz[39], L.Lyons[34], G.Maehlum[15], J.Maillard[6], A.Maio[20], A.Maltezos[9], F.Mandl[50], J.Marco[41], B.Marechal[47], M.Margoni[35], J-C.Marin[7], C.Mariotti[40], A.Markou[9], T.Maron[52], S.Marti[49], C.Martinez-Rivero[41], F.Martinez-Vidal[49], F.Matorras[41], C.Matteuzzi[27], G.Matthiae[38], M.Mazzucato[35], M.Mc Cubbin[21], R.Mc Kay[1], R.Mc Nulty[21], J.Medbo[48], C.Meroni[27], W.T.Meyer[1], M.Michelotto[35], E.Migliore[45], I.Mikulec[50], L.Mirabito[24], W.A.Mitaroff[50], G.V.Mitselmakher[14], U.Mjoernmark[23], T.Moa[44], R.Moeller[28], K.Moenig[7], M.R.Monge[11], P.Morettini[11], H.Mueller[15], W.J.Murray[37], B.Muryn[16], G.Myatt[34], F.Naraghi[12], F.L.Navarria[5], P.Negri[27], S.Nemecek[10], W.Neumann[52], R.Nicolaidou[3], B.S.Nielsen[28], V.Nikolaenko[24], P.Niss[44], A.Nomerotski[35], A.Normand[34], V.Obraztsov[42], A.G.Olshevski[14], R.Orava[13], K.Osterberg[13], A.Ouraou[39], P.Paganini[18], M.Paganoni[27], R.Pain[22], H.Palka[16], Th.D.Papadopoulou[31], L.Pape[7], F.Parodi[11], A.Passeri[40], M.Pegoraro[35], J.Pennanen[13], L.Peralta[20], V.Perevozchikov[42], H.Pernegger[50], M.Pernicka[50], A.Perrotta[5], C.Petridou[46], A.Petrolini[11], H.T.Phillips[37], G.Piana[11], F.Pierre[39], M.Pimenta[20], S.Plaszczynski[18], O.Podobrin[15], M.E.Pol[17], G.Polok[16], P.Poropat[46], V.Pozdniakov[14], M.Prest[46], P.Privitera[38], A.Pullia[27], D.Radojicic[34], S.Ragazzi[27], H.Rahmani[31], J.Rames[10], P.N.Ratoff[19], A.L.Read[32], M.Reale[52], P.Rebecchi[18], N.G.Redaelli[27], M.Regler[50], D.Reid[7], P.B.Renton[34], L.K.Resvanis[3], F.Richard[18], J.Richardson[21], J.Ridky[10], G.Rinaudo[45], I.Ripp[39], A.Romero[45], I.Roncagliolo[11], P.Ronchese[35], L.Roos[12], E.I.Rosenberg[1], E.Rosso[7], P.Roudeau[18], T.Rovelli[5], W.Ruckstuhl[30], V.Ruhlmann-Kleider[39], A.Ruiz[41], H.Saarikko[13], Y.Sacquin[39], G.Sajot[12], J.Salt[49], J.Sanchez[25], M.Sannino[11],

S.Schael[7], H.Schneider[15], M.A.E.Schyns[52], G.Sciolla[45], F.Scuri[46], A.M.Segar[34], A.Seitz[15], R.Sekulin[37], R.Seufert[15], R.C.Shellard[36], I.Siccama[30], P.Siegrist[39], S.Simonetti[39], F.Simonetto[35], A.N.Sisakian[14], T.B.Skaali[32], G.Smadja[24], N.Smirnov[42], O.Smirnova[14], G.R.Smith[37], R.Sosnowski[51], D.Souza-Santos[36], T.Spassov[20], E.Spiriti[40], S.Squarcia[11], H.Staeck[52], C.Stanescu[40], S.Stapnes[32], I.Stavitski[35], G.Stavropoulos[9], K.Stepaniak[51], F.Stichelbaut[7], A.Stocchi[18], J.Strauss[50], J.Straver[7], R.Strub[8], B.Stugu[4], M.Szczekowski[51], M.Szeptycka[51], T.Tabarelli[27], O.Tchikilev[42], G.E.Theodosiou[9], Z.Thome[47], A.Tilquin[26], J.Timmermans[30], V.G.Timofeev[14], L.G.Tkatchev[14], T.Todorov[8], D.Z.Toet[30], A.Tomaradze[2], B.Tome[20], E.Torassa[45], L.Tortora[40], G.Transtromer[23], D.Treille[7], W.Trischuk[7], G.Tristram[6], C.Troncon[27], A.Tsirou[7], E.N.Tsyganov[14], M-L.Turluer[39], T.Tuuva[13], I.A.Tyapkin[22], M.Tyndel[37], S.Tzamarias[21], B.Ueberschaer[52], S.Ueberschaer[52], O.Ullaland[7], V.Uvarov[42], G.Valenti[5], E.Vallazza[7], J.A.Valls Ferrer[49], C.Vander Velde[2], G.W.Van Apeldoorn[30], P.Van Dam[30], M.Van Der Heijden[30], W.K.Van Doninck[2], J.Van Eldik[30], P.Vaz[7], G.Vegni[27], L.Ventura[35], W.Venus[37], F.Verbeure[2], M.Verlato[35], L.S.Vertogradov[14], D.Vilanova[39], P.Vincent[24], L.Vitale[46], E.Vlasov[42], A.S.Vodopyanov[14], M.Vollmer[52], M.Voutilainen[13], V.Vrba[10], H.Wahlen[52], C.Walck[44], F.Waldner[46], A.Wehr[52], M.Weierstall[52], P.Weilhammer[7], A.M.Wetherell[7], J.H.Wickens[2], M.Wielers[15], G.R.Wilkinson[34], W.S.C.Williams[34], M.Winter[8], M.Witek[7], G.Wormser[18], K.Woschnagg[48], K.Yip[34], O.Yushchenko[42], F.Zach[24], A.Zaitsev[42], A.Zalewska[16], P.Zalewski[51], D.Zavrtanik[43], E.Zevgolatakos[9], N.I.Zimin[14], M.Zito[39], D.Zontar[43], R.Zuberi[34], G.Zumerle[35]

[1] Ames Laboratory and Department of Physics, Iowa State University, Ames IA 50011, USA
[2] Physics Department, Univ. Instelling Antwerpen, Universiteitsplein 1, B-2610 Wilrijk, Belgium
and IIHE, ULB-VUB, Pleinlaan 2, B-1050 Brussels, Belgium
and Faculté des Sciences, Univ. de l'Etat Mons, Av. Maistriau 19, B-7000 Mons, Belgium
[3] Physics Laboratory, University of Athens, Solonos Str. 104, GR-10680 Athens, Greece
[4] Department of Physics, University of Bergen, Allégaten 55, N-5007 Bergen, Norway
[5] Dipartimento di Fisica, Università di Bologna and INFN, Via Irnerio 46, I-40126 Bologna, Italy
[6] Collège de France, Lab. de Physique Corpusculaire, IN2P3-CNRS, F-75231 Paris Cedex 05, France
[7] CERN, CH-1211 Geneva 23, Switzerland
[8] Centre de Recherche Nucléaire, IN2P3 - CNRS/ULP - BP20, F-67037 Strasbourg Cedex, France
[9] Institute of Nuclear Physics, N.C.S.R. Demokritos, P.O. Box 60228, GR-15310 Athens, Greece
[10] FZU, Inst. of Physics of the C.A.S. High Energy Physics Division, Na Slovance 2, 180 40, Praha 8, Czech Republic
[11] Dipartimento di Fisica, Università di Genova and INFN, Via Dodecaneso 33, I-16146 Genova, Italy
[12] Institut des Sciences Nucléaires, IN2P3-CNRS, Université de Grenoble 1, F-38026 Grenoble Cedex, France
[13] Research Institute for High Energy Physics, SEFT, P.O. Box 9, FIN-00014 Helsinki, Finland
[14] Joint Institute for Nuclear Research, Dubna, Head Post Office, P.O. Box 79, 101 000 Moscow, Russian Federation
[15] Institut für Experimentelle Kernphysik, Universität Karlsruhe, Postfach 6980, D-76128 Karlsruhe, Germany
[16] High Energy Physics Laboratory, Institute of Nuclear Physics, Ul. Kawiory 26a, PL-30055 Krakow 30, Poland
[17] Centro Brasileiro de Pesquisas Físicas, rua Xavier Sigaud 150, BR-22290 Rio de Janeiro, Brazil
[18] Université de Paris-Sud, Lab. de l'Accélérateur Linéaire, IN2P3-CNRS, Bat 200, F-91405 Orsay Cedex, France
[19] School of Physics and Materials, University of Lancaster, Lancaster LA1 4YB, UK
[20] LIP, IST, FCUL - Av. Elias Garcia, 14-1°, P-1000 Lisboa Codex, Portugal
[21] Department of Physics, University of Liverpool, P.O. Box 147, Liverpool L69 3BX, UK
[22] LPNHE, IN2P3-CNRS, Universités Paris VI et VII, Tour 33 (RdC), 4 place Jussieu, F-75252 Paris Cedex 05, France
[23] Department of Physics, University of Lund, Sölvegatan 14, S-22363 Lund, Sweden
[24] Université Claude Bernard de Lyon, IPNL, IN2P3-CNRS, F-69622 Villeurbanne Cedex, France
[25] Universidad Complutense, Avda. Complutense s/n, E-28040 Madrid, Spain
[26] Univ. d'Aix - Marseille II - CPP, IN2P3-CNRS, F-13288 Marseille Cedex 09, France
[27] Dipartimento di Fisica, Università di Milano and INFN, Via Celoria 16, I-20133 Milan, Italy
[28] Niels Bohr Institute, Blegdamsvej 17, DK-2100 Copenhagen 0, Denmark
[29] NC, Nuclear Centre of MFF, Charles University, Areal MFF, V Holesovickach 2, 180 00, Praha 8, Czech Republic
[30] NIKHEF-H, Postbus 41882, NL-1009 DB Amsterdam, The Netherlands
[31] National Technical University, Physics Department, Zografou Campus, GR-15773 Athens, Greece
[32] Physics Department, University of Oslo, Blindern, N-1000 Oslo 3, Norway
[33] Dpto. Fisica, Univ. Oviedo, C/P. Pérez Casas, S/N-33006 Oviedo, Spain
[34] Department of Physics, University of Oxford, Keble Road, Oxford OX1 3RH, UK
[35] Dipartimento di Fisica, Università di Padova and INFN, Via Marzolo 8, I-35131 Padua, Italy
[36] Depto. de Fisica, Pontificia Univ. Católica, C.P. 38071 RJ-22453 Rio de Janeiro, Brazil
[37] Rutherford Appleton Laboratory, Chilton, Didcot OX11 OQX, UK
[38] Dipartimento di Fisica, Università di Roma II and INFN, Tor Vergata, I-00173 Rome, Italy
[39] Centre d'Etude de Saclay, DSM/DAPNIA, F-91191 Gif-sur-Yvette Cedex, France
[40] Istituto Superiore di Sanità, Ist. Naz. di Fisica Nucl. (INFN), Viale Regina Elena 299, I-00161 Rome, Italy
[41] C.E.A.F.M., C.S.I.C. - Univ. Cantabria, Avda. los Castros, S/N-39006 Santander, Spain, (CICYT-AEN93-0832)
[42] Inst. for High Energy Physics, Serpukov P.O. Box 35, Protvino, (Moscow Region), Russian Federation
[43] J. Stefan Institute and Department of Physics, University of Ljubljana, Jamova 39, SI-61000 Ljubljana, Slovenia
[44] Fysikum, Stockholm University, Box 6730, S-113 85 Stockholm, Sweden
[45] Dipartimento di Fisica Sperimentale, Università di Torino and INFN, Via P. Giuria 1, I-10125 Turin, Italy
[46] Dipartimento di Fisica, Università di Trieste and INFN, Via A. Valerio 2, I-34127 Trieste, Italy
and Istituto di Fisica, Università di Udine, I-33100 Udine, Italy
[47] Univ. Federal do Rio de Janeiro, C.P. 68528 Cidade Univ., Ilha do Fundão BR-21945-970 Rio de Janeiro, Brazil
[48] Department of Radiation Sciences, University of Uppsala, P.O. Box 535, S-751 21 Uppsala, Sweden
[49] IFIC, Valencia-CSIC, and D.F.A.M.N., U. de Valencia, Avda. Dr. Moliner 50, E-46100 Burjassot (Valencia), Spain
[50] Institut für Hochenergiephysik, Österr. Akad. d. Wissensch., Nikolsdorfergasse 18, A-1050 Vienna, Austria
[51] Inst. Nuclear Studies and University of Warsaw, Ul. Hoza 69, PL-00681 Warsaw, Poland
[52] Fachbereich Physik, University of Wuppertal, Postfach 100 127, D-42097 Wuppertal 1, Germany

1 Introduction

The concept of mixing was first introduced to describe the quantum mechanical evolution of the neutral kaon system [1]. A formal analogy exists with the $B^0 - \bar{B}^0$ system, where, in absence of CP violation, the flavour eigenstates B^0 and $\bar{B}^0$ are related to the mass eigenstates B_1 and B_2,

$$B^0 = \frac{B_1 + B_2}{\sqrt{2}} \qquad \bar{B}^0 = \frac{B_1 - B_2}{\sqrt{2}}.$$

Neglecting the decay width difference of the mass eigenstates, the probability that a generated B^0 meson stays as B^0 at time t is given by:

$$P(B^0 \to B^0) = \frac{e^{-\frac{\Gamma t}{\hbar}}}{2\tau_B}\left[1 + cos\left(\frac{\Delta m\ t}{\hbar}\right)\right], \tag{1}$$

and the probability that it oscillates into $\bar{B}^0$ at time t is:

$$P(B^0 \to \bar{B}^0) = \frac{e^{-\frac{\Gamma t}{\hbar}}}{2\tau_B}\left[1 - cos\left(\frac{\Delta m\ t}{\hbar}\right)\right], \tag{2}$$

where Γ is the decay width, τ_B is the B lifetime, Δm is the magnitude of the mass difference of the two eigenstates and the total time integrated probability that a B^0 mixes into a $\bar{B}^0$ is:

$$\chi = \frac{1}{2}\frac{\left(\frac{\Delta m}{\Gamma}\right)^2}{1 + \left(\frac{\Delta m}{\Gamma}\right)^2}. \tag{3}$$

This is valid both for the B_d^0 and B_s^0 mesons. However, the B_s^0 oscillation frequency is expected to be quite large, and the measurement of its time dependence requires high statistics and very good proper time reconstruction. From the average of the existing measurements [2] of the time integrated B_d^0 mixing at the $\Upsilon(4S)$, $\Delta m/\Gamma = 0.69 \pm 0.10$, a complete oscillation period is expected to take about 9 B_d^0 lifetimes, corresponding to about 2 cm decay length at LEP energies. Thus, the DELPHI decay length resolution, better than 500 μm, is well suited to observe the B_d^0 time dependent oscillation. Measurements of time dependent B_d^0 mixing have also been made by the ALEPH [3] and OPAL [4] collaborations.

2 The DELPHI detector

Only the components of the DELPHI detector which play an important role in the present analysis are described here. A complete description of the DELPHI apparatus is given in [5].

The central tracking system, comprising the inner detector (ID), the time projection chamber (TPC) and the outer detector (OD), measures the charged particle tracks at polar angles between 30° and 150°. Combining the information from these detectors with that from the microvertex detector (VD), a resolution $\sigma(p)/p$ of 3.5 % has been obtained for muons of 45 GeV/c momentum. The TPC, the main tracking device, is a cylinder of 30 cm inner radius, 122 cm outer radius and length 2.7 m. For polar angles between 39° and 141° it provides up to 16 space points along the charged particle trajectory. The

energy loss (dE/dx) for each charged particle is measured by the 192 TPC sense wires as the truncated mean of the smallest 80% of the wire signals. Using $Z^0 \to \mu^+\mu^-$ events, the dE/dx resolution has been measured to be 5.5%. For particles in hadronic jets the resolution is 7.5%, but for 25% of the particles the dE/dx is not measured due to the presence of another charged particle within the two-track resolution distance of the TPC in the direction parallel to the beam.

The microvertex detector [6] is made of three concentric shells of silicon-strip detectors at radii of 6.3, 9 and 11 cm covering the central region of the DELPHI apparatus at polar angles between 27° and 153°. The shells surround the beam pipe, a beryllium cylinder 1.45 mm thick with a 5.3 cm inner radius. Each shell consists of 24 modules with about 10% overlap in azimuth between the modules. Each module holds 4 detectors with strips parallel to the beam direction. The silicon detectors are 300 μm thick and have a strip pitch of 25 μm, every other strip being read out. The read-out strips (50 μm pitch) are AC-coupled and give a 5 μm intrinsic precision on the coordinates of the charged particle tracks transverse to the beam direction. After a careful procedure of relative alignment of each single detector, an overall precision of 8 μm per point has been achieved.

3 D^* Selection

Multihadronic decays of the Z^0 were selected as described in an earlier paper [10]. For the present analysis the decay $D^{*+} \to D^0\pi^+$ followed by $D^0 \to K^-\pi^+$ was used, as well as its charge conjugate. The selection criteria rely mainly on the small mass difference between D^* and D^0 mesons. All pairs of charged particles of opposite sign with a momentum greater than 1 GeV/c were combined and an invariant mass was calculated assigning in turn the kaon or the pion mass. The $D^{*\pm}$ mass was then computed by adding all possible pions with momentum between 0.4 GeV/c and 4.5 GeV/c and with a charge opposite to that of the kaon candidate. The energy of the $D^{*\pm}$ divided by the beam energy ($X_E = E_{D^*}/E_{beam}$) was required to be greater than 0.15 and the mass of the (Kπ) candidates to lie between 1.79 and 1.94 GeV/c^2 for $X_E > 0.25$ or between 1.82 and 1.90 GeV/c^2 for $0.15 < X_E < 0.25$.

The $D^{*\pm}$ mesons coming from $b\bar{b}$ events have a softer energy spectrum than those coming from $c\bar{c}$ events. About 50% of the $D^{*\pm}$ coming from $c\bar{c}$ were rejected by requiring $X_E < 0.5$ whereas about 90% of the $D^{*\pm}$ from $b\bar{b}$ were kept.

To reduce the combinatorial background the cosine of the angle θ^* between the D^0 flight direction and the kaon direction in the D^0 rest frame was required to be greater than -0.8 for $0.25 < X_E < 0.50$ and greater than -0.6 for $0.15 < X_E < 0.25$. The tighter cuts on the mass of the (Kπ) candidates and on $\cos\theta^*$ for $0.25 < X_E < 0.50$ were used because the combinatorial background is more important in this X_E range. The distribution of the mass difference $\Delta M = M(K^-\pi^+\pi^+) - M(K^-\pi^+)$ obtained by applying the above selection criteria to about 1.7 million hadronic Z^0 decays collected during 1991-1993 is shown in Fig. 1. In the range of ΔM between 0.1435 and 0.1475 GeV/c^2, which contains most of the signal, 2637 events were observed, which correspond to a D^* signal of 1491 ± 51 events, after subtraction of the combinatorial background.

All charged particles with an impact parameter of less than 2 mm relative to the beam position in the plane transverse to the beam direction were used to reconstruct the primary vertex. The known position of the beam spot was used as a constraint. If the primary vertex fit had a χ^2-probability less than 10^{-3}, an iterative procedure was applied which removed the track contributing most to the χ^2 at each iteration. In a Monte Carlo

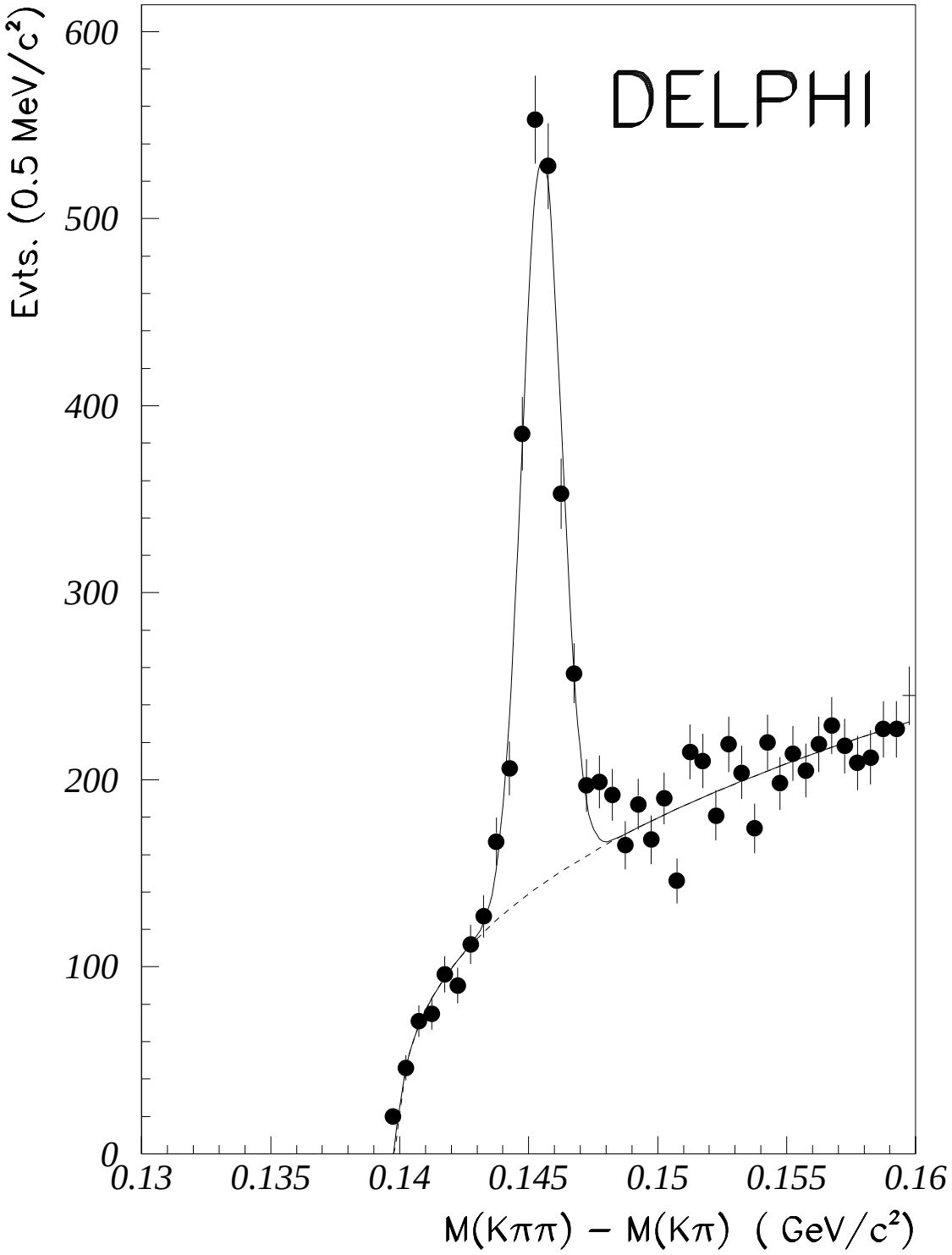

Figure 1: Distribution of $\Delta M = M(K^-\pi^+\pi^+) - M(K^-\pi^+)$

simulated $b\bar{b}$ sample, this procedure was found to reconstruct vertices with an accuracy of 80 μm in the horizontal direction, where the beam spot has the larger spread, and 40 μm vertically.

The $K^-\pi^+\pi^+$ combination was used to compute the secondary vertex which in practice, due to the kinematics of the decay, coincides with the D^0 decay point. The distance between the primary and the secondary vertices was calculated in the transverse plane. This distance was signed according to the sign of the scalar product of the D momentum vector and the vector joining the primary to the secondary vertices. Then, the decay length, d, was determined in space by using the D meson direction. The average resolution on the decay length was found to be 300 μm from a Monte Carlo study.

4 D^* - Hemisphere charge correlation

The measurement of B_d^0-$\bar{B}_d^0$ mixing involves the tagging of the presence of a b or a $\bar{b}$ quark in a given hemisphere at the time of production and the identification of a $\bar{B}_d^0$ or a B_d^0 particle at the time of its decay.

The charge of the D^* coming from a neutral B meson decay tags the flavour at the time of decay, since B_d^0 mainly produces D^{*-} and $\bar{B}_d{}^0$ mainly produces D^{*+}.

The neutral B flavour at the time of production can be inferred from the variable C_H, computed for each hemiphere and defined as:

$$C_H = \frac{\sum_i (\vec{p_i} \ . \ \vec{e_s})^k q_i}{\sum_i (\vec{p_i} \ . \ \vec{e_s})^k}, \tag{4}$$

where $\vec{e_s}$ is the unit vector of the sphericity axis, $\vec{p_i}$ and q_i are the momentum and the charge of track i. A value of 0.6 was chosen for the weight power factor k [7].

The hemisphere charge, determinated from simulated events, has a quite broad distribution, with a mean value close to the charge of the quark from which the jet originated. The probability ϵ of correctly identifying a b ($\bar{b}$) quark by requiring a negative (positive) hemisphere charge was found to be 0.628 ± 0.008 from simulation [8]. This is an average value, since the probability of correctly tagging of the b charge is slightly different for b producing B_d^0, $B^{\pm}$, B_s^0 and Λ_b.

If the B^0 meson decaying into a D^* has (not) mixed, the D^* charge and the charge of the hemisphere opposite to the D^* should be of unlike (like) sign. The effect of incorrect charge identification reduces the amplitude of the observable time dependent oscillation, as shown in the charge correlation function Q :

$$Q(t) = \frac{N_{like} - N_{unlike}}{N_{like} + N_{unlike}} = (2\epsilon - 1) \ cos \left(\frac{\Delta m \ t}{\hbar} \right). \tag{5}$$

In order to improve the charge tagging, the hemisphere containing the D^* was also used. The difference ΔC_H between the charge of the hemisphere opposite to the D^* and the charge of the hemisphere containing the D^* was calculated and compared with the charge of the D^*. An event was considered as unlike sign when ΔC_H was opposite in sign to the D^* charge. In this case, the D^* was interpreted as originating from a B^0 meson having undergone a mixing.

The probability ϵ^{unlike} of classifying a reconstructed D^* event in the unlike sign category was determined from a data set of generated Z^0 events [8], passed through a detailed simulation of the detector [9]. The corresponding probability for an event to be classified in the like sign sample , ϵ^{like}, is simply given by $\epsilon^{like} = 1$ - ϵ^{unlike}.

In Table 1 the various sources of D^* events are summarized, with their expected contribution relative to the fraction of the $B_d^0 \to D^{*-}X$ decay. For each source the probability to assign it to the unlike sign events sample is given. The quoted values of the ϵ^{unlike} probabilities were obtained after applying the event selection described in Section 3. The quoted uncertainty comes from the limited statistics of the simulation.
For D^* originating from the decay of a B^0 meson, the probability depends on whether the B^0 mixed or not:

$$\begin{aligned} \epsilon_{mix}^{unlike} &= 0.532 \pm 0.024, \\ \epsilon_{unmix}^{unlike} &= 0.275 \pm 0.010, \end{aligned}$$

where ϵ_{mix}^{unlike} is the probability to tag correctly a $B^0 - \bar{b}$ (or $\bar{B}^0 - b$) event where the B^0 meson has oscillated as unlike sign and $\epsilon_{unmix}^{unlike}$ is the probability to tag a $B^0 - b$ (or $\bar{B}^0 - \bar{b}$) event where the B^0 meson has not oscillated as unlike sign. This latter class of events would naturally contribute to the like-sign category, the probability for these events to be classified as like-sign being $\epsilon_{unmix}^{like} = 1$ - $\epsilon_{unmix}^{unlike} = 0.725$. Notice that the probability of correctly tagging the sign depends on whether or not the B^0 has mixed, due to the fact that the jet charge in the D^* hemisphere was used.

Charged $B^{\mp}$ mesons can decay into $D^{*\pm}$; however, there is no experimental measurement of the corresponding decay rate. The fraction of $B^{\mp}$ decaying into $D^{*\pm}$ used in the simulation, normalized to all the B decaying into $D^{*\pm}$, is 0.17 and

$$\epsilon_{B^{\mp}}^{unlike} = 0.239 \pm 0.018$$

where $\epsilon_{B^{\mp}}^{unlike}$ is the probability to tag an event where a $D^{*\pm}$ comes from a $B^{\mp}$ decay in the unlike sign category.

Also, D^* from $c\bar{c}$ events must be considered. The probability $\epsilon_{c\bar{c}}^{unlike}$ of tagging a $c\bar{c}$ event as unlike sign was found to be:

$$\epsilon_{c\bar{c}}^{unlike} = 0.601 \pm 0.010$$

Minor contributions can come from the Cabibbo suppressed decays in which a virtual W^- couples to $c\bar{d}$ giving rise to decay such $B_d^0 \to D^{*+}X$ and $B^+ \to D^{*+}X$ with an opposite correlation between the charges of the B and of the D^* mesons. Contributions from B baryons were neglected.

5 Probability distributions and fitting procedure

For each class of event in Table 1, the expected time distribution corresponding to the secondary D^0 vertices was found. They were obtained by convoluting the theoretical proper time distributions with Gaussian functions to account for the experimental accuracy in the proper time evaluation.

The B^0 proper time, $t_B = m_B d_B / p_B$, where m_B, d_B and p_B are the B^0 mass, decay distance and momentum, could not be measured directly, since the measured decay distance is the sum of the B^0 and of the D^0 decay distances, $d = d_B + d_D$. To take into account the D^0 flight, a new variable was defined for each event, which is the sum of the B^0 and D^0 proper times, $t = t_B + t_D$. The probability distributions for the variable t, $P_{unsmeared}^{mix(unmix)}(t, \Delta m)$, were obtained by convoluting the time dependent probability distributions (1) and (2) with the exponential D^0 decay distribution $e^{-t_D/\tau_D}/\tau_D$, where τ_D is the D^0 lifetime.

Table 1: Estimates from simulation of different contributions to the D^* sample with their relative importance. The initial fractions of different B hadrons are the ones assumed in the Monte Carlo [9]. These contributions are classified as like or unlike sign events assuming an exact tag of the original B meson. The ϵ^{unlike} probability is also given and the quoted uncertainty comes from the limited statistics of the simulation . The quoted values were obtained after applying the event selection described in Section 3.

like sign	unlike sign	relative fraction	ϵ^{unlike}
$B_d^0 \to D^{*-}X$		1.	0.275 ± 0.010
	$B_d^0 \to \bar{B}_d^0 \to D^{*+}X$	0.22	0.532 ± 0.024
$B^+ \to D^{*-}X$		0.28	0.239 ± 0.018
	$c\bar{c} : \bar{c} \to D^{*-}X$	0.93	0.601 ± 0.010
	$B_d^0 \to D^{*+}X$	0.03	0.500 ± 0.071
	$B^+ \to D^{*+}X$	0.04	0.657 ± 0.057
$B_s^0 \to D^{*-}X$		0.04	0.284 ± 0.052
	$B_s^0 \to \bar{B}_s^0 \to D^{*+}X$	0.04	0.605 ± 0.054

The sum of B^0 and D^0 proper times can be written as:

$$t = t_B + t_D = \frac{m_B}{p_B} d_B + \frac{m_D}{p_D} d_D = \frac{m_B}{p_B} d + \left(\frac{m_D}{p_D} - \frac{m_B}{p_B} \right) d_D \simeq \frac{m_B}{p_B} d, \qquad (6)$$

where the term proportional to d_D has been neglected, being of order of a percent with respect to the other term . The B^0 momentum in equation (6) was taken as the mean fraction of the beam energy carried by the B^0. It was checked with the Monte Carlo simulation that the average fraction of beam energy taken by the B^0 is almost unaffected by the D^* selection criteria. Also, a parametrization of the B^0 momentum as a function of the reconstructed D^* momentum was studied. The resolution on t slightly improves by using such parametrization, but the effect on the measurement of Δm was found to be negligible. Thus, the simpler approximation of the average B^0 momentum, $p_B \simeq 0.7 E_{beam}$, was used. The validity of the approximations involved in equation (6) was verified on a set of generated B^0 events [8], passed through a detailed simulation of the detector. The average resolution on t was found to be 0.4 ps, which was sufficient for the measurement of the time dependent B_d^0 mixing. The final normalized probability distributions $P_{B^0}^{mix(unmix)}(t, \Delta m)$ were obtained by convoluting the probabilities $P_{unsmeared}^{mix(unmix)}(t, \Delta m)$ with a Gaussian resolution distribution of standard deviation $\sigma_t = \left[(\sigma_d/d)^2 + (\sigma_{p_{B^0}}/p_{B^0})^2 \right]^{\frac{1}{2}} t$. An average value for $\sigma_{p_{B^0}}/p_{B^0} = 0.17$ was used as determined from the simulation. The choice of a gaussian $\sigma_{p_{B^0}}$ does not describe properly the B^0 momentum distribution error, but this approximation is adequate for the performed measurement.

For charged B mesons, the normalized probability distribution $P_{B^\mp}(t)$ was determined in a similar way as for $P_{B^0}^{mix(unmix)}(t, \Delta m)$ but without including the oscillation terms of the expressions (1) and (2).

When the D^* originates from a $c\bar{c}$, the variable t previously defined differs from the D^0 proper time by the ratio of the D^0 over the B^0 boost. The corresponding time distribution $P_{c\bar{c}}(t)$ was determined from the Monte Carlo simulation and parametrized with an exponential and two Gaussian distributions.

The time distribution corresponding to the events from the combinatorial background under the D^* peak, $P_{comb}(t)$, was obtained from the upper sideband of the $\Delta M = M(K\pi\pi) - M(K\pi)$ mass distribution, by requiring $\Delta M > 0.15$ GeV/c^2. The possibility of a time dependent oscillating contribution to the combinatorial background was studied by comparing the ratio of the time distributions of unlike to like sign events. No evidence for such a contribution was found, and the same distribution $P_{comb}(t)$ was used for like and unlike sign events.

An unbinned maximum likelihood method was used to fit the time distributions for the unlike and like sign events. The likelihood function for unlike sign events was written as:

$$\begin{aligned} \mathcal{L}^{unlike} &= f_{B^0}\left[\epsilon^{unlike}_{mix} P^{mix}_{B^0}(t,\Delta m) + \epsilon^{unlike}_{unmix} P^{unmix}_{B^0}(t,\Delta m)\right] + \\ & f_{B^\pm}\epsilon^{unlike}_{B^\pm} P_{B^\pm}(t) + f_{c\bar{c}}\epsilon^{unlike}_{c\bar{c}} P_{c\bar{c}}(t) + f_{comb}\epsilon^{unlike}_{comb} P_{comb}(t), \end{aligned} \tag{7}$$

- f_{B^0}, $f_{B^\pm}$, $f_{c\bar{c}}$ and f_{comb} are the fractions of B^0, $B^\pm$, $c\bar{c}$ and of the combinatorial background in the selected sample of events,
- ϵ^{unlike}_{mix} is the probability of tagging a mixed B^0 as an unlike sign event,
- $\epsilon^{unlike}_{unmix}$ is the probability of tagging an unmixed B^0 as an unlike sign event,
- $\epsilon^{unlike}_{B^\pm, c\bar{c}, comb}$ are the probabilities of tagging a $B^\pm$, $c\bar{c}$ and combinatorial background events as unlike sign candidate.

The contribution from B^0_s mesons was found to be negligible (see Table 1) and not considered in the likelihood function.

The likelihood function for like sign events $\mathcal{L}^{like}$ is obtained by substituting all the efficiencies ϵ in (7) by $(1-\epsilon)$. The values used for the different parameters in (7) are given in Section 6.

The expected behaviour of the charge correlation Q for a pure B^0_d sample generated with $\Delta m = 0.50\ \hbar/ps$ is shown in Fig. 2 as a full curve. The charge correlation is plotted as a function of the measured decay length, which is equivalent to t having chosen a fixed value for the B momentum. Notice that the oscillating behaviour of the charge correlation function Q is not expected to be symmetric around zero, since the probabilities for correct charge tagging are different for mixed and unmixed events. The effect of the inclusion of charged B, charm and combinatorial background results in a damping of the amplitude of the oscillation, as shown by the dashed curve in Fig. 2. The charm and combinatorial background, having a small effective lifetime, mostly contribute in the damping of the oscillation at small decay length.

6 Experimental results and consistency checks

The amplitude of the time dependent oscillation is sensitive to the probability of correctly tagging events with unmixed and mixed B^0, as discussed in Section 4. For this reason, in order to be insensitive to details of the Monte Carlo simulation, the maximum likelihood fit was performed leaving free Δm and one of the probabilities, $\epsilon^{unlike}_{unmix}$, and fixing the parameters f_{comb} , ϵ^{unlike}_{comb}, τ_B , $f_{c\bar{c}}$ and the effective time distribution for background events to the values obtained from the data. The values of ϵ^{unlike}_{mix}, $\epsilon^{unlike}_{B^\mp}$ and $\epsilon^{unlike}_{c\bar{c}}$ were taken from the simulation, according to Table 1, as well as $f_{B^\mp}$ and the effective time distribution of charm events.

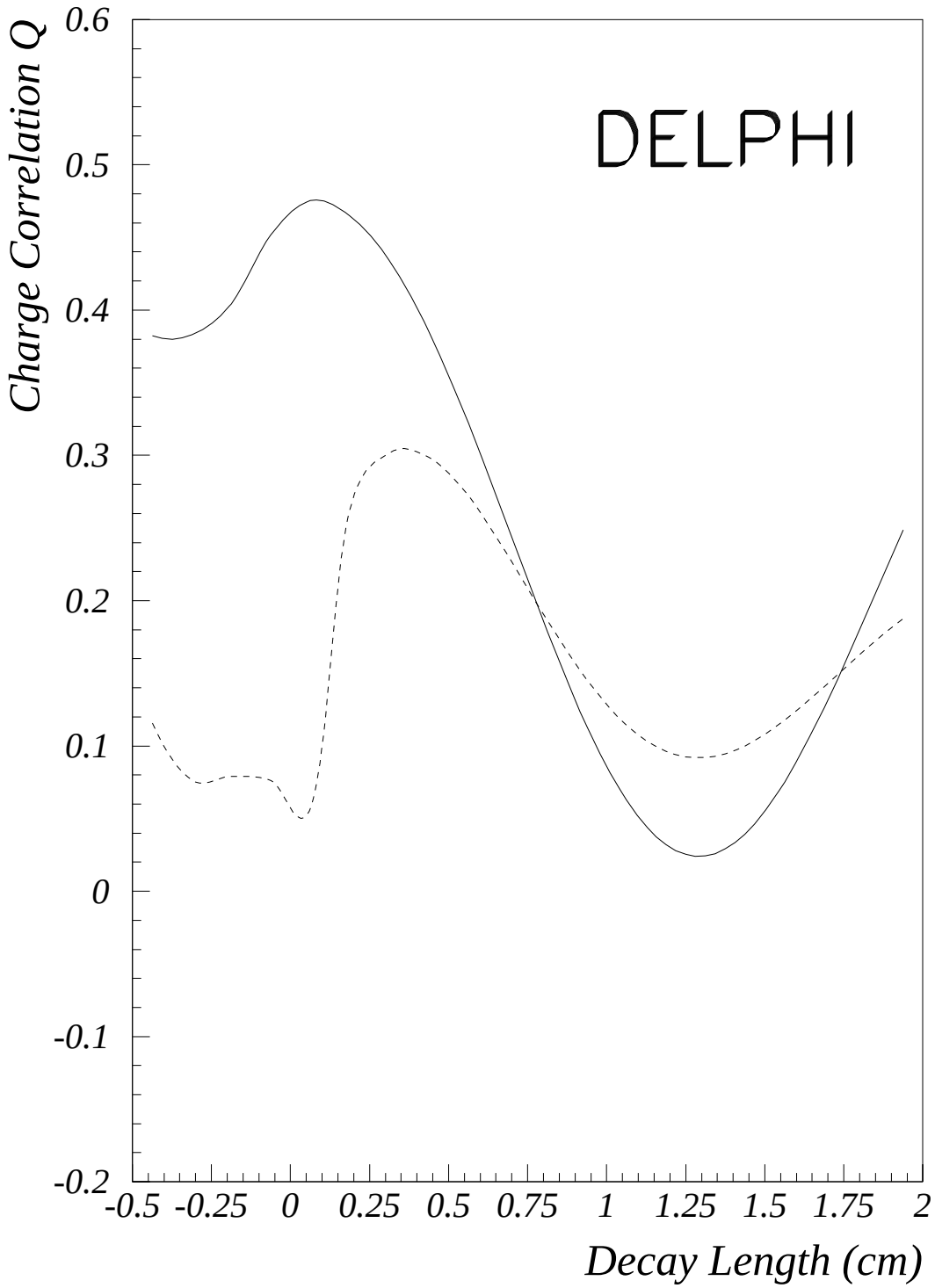

Figure 2: The charge correlation $Q(t)$ as a function of the D^0 decay length. The full curve corresponds to the expected behaviour for B_d^0 events generated with $\Delta m = 0.50\ \hbar/ps$. The dashed curve includes the contribution from charged B, charm and combinatorial background.

In order to enhance the signal to background ratio , events were required to have ΔM between 0.1445 and 0.1465 GeV/c^2, leaving 1816 events. The fraction of combinatorial background, f_{comb} , was obtained from a fit of the ΔM spectrum which was parametrized with a Gaussian distribution for the signal and a smooth polynomial for the background. The measured fraction of background events in the candidate sample was $f_{comb} = 0.318 \pm 0.020$. Events having $\Delta M > 0.15$ GeV/c^2 were used to measure $\epsilon_{comb}^{unlike} = 0.481 \pm 0.008$.
The fraction of D^* originating from charm quark fragmentation in the sample, $r_{c\bar{c}} = \frac{f_{c\bar{c}}}{f_{c\bar{c}}+f_{b\bar{b}}}$, was obtained from a study of the X_E distribution. The measured X_E distribution was fitted to a sum of the distributions for b and c events, taken from the simulation. From the relative importance of the two contributions, the fraction of charm events was measured to be $r_{c\bar{c}} = 0.36 \pm 0.05 \pm 0.03$, in agreement with the expectation $r_{c\bar{c}} = 0.36$ from the simulation.

The B^0 momentum approximated by the average fraction of beam energy carried by the B^0, as explained in Sect. 5, was fixed to the value measured by DELPHI, $X_B = 0.695 \pm 0.03 \pm 0.01$ [11].

The B lifetime was obtained from the data. A fit was performed assuming the charm and background time distributions and fractions previously determined and τ_B =1.63±0.10 ps was found.

Using these parameters , the result of the fit was:

$$\begin{aligned} \Delta m &= 0.50 \pm 0.12(stat)\ \hbar/ps \\ \epsilon_{unmix}^{unlike} &= 0.271 \pm 0.036. \end{aligned}$$

The fitted value of $\epsilon_{unmix}^{unlike}$ is in good agreement with the expectation of 0.275 from the simulation. The experimental distribution of the charge correlation function Q is shown in Fig. 3, with the result of the fit to the like and unlike sign distributions superimposed. Also shown as a dashed curve is the result of a fit to a time independent mixing hypothesis. The time independent mixing hypothesis was tested assuming a simple exponential decay time distribution for $P_{B^0}^{mix}$ and $P_{B^0}^{unmix}$ in the likelihood functions. The relative proportion of mixed and unmixed events was taken into account fixing $\chi = 0.17$, according to the existing measurements of the time integrated B_d^0 mixing. The negative log likelihood increased by 4.3 which corresponds to 2.9 standard deviations.

Several checks were performed on the analysis procedure.

- Fixing Δm to the fitted value of 0.50 $\hbar/ps$, the two B^0 unlike sign probabilities were fitted. The following values were found: $\epsilon_{unmix}^{unlike} = 0.264 \pm 0.036$ and $\epsilon_{mix}^{unlike} = 0.569 \pm 0.087$. The latter value is in good agreement with expectation of 0.532 from simulation.

- An estimate of $\epsilon_{c\bar{c}}^{unlike}$ was obtained from the data in the following way. The events rejected by the cut $X_E > 0.50$ are enriched in $c\bar{c}$ events ($\simeq 80\%$). From the number of unlike sign events with $X_E > 0.50$ in this sample and using the charge correlation efficiencies from simulation for non-charm events, $\epsilon_{c\bar{c}}^{unlike} = 0.58 \pm 0.02$ was obtained, to be compared to the expectation of 0.61 ± 0.01 from simulation.

- The fraction of $c\bar{c}$ events was left free in the fit, and $r_{c\bar{c}} = 0.280 \pm 0.054$ was obtained in agreement with the aforementioned measured value of $0.36 \pm 0.05 \pm 0.03$.

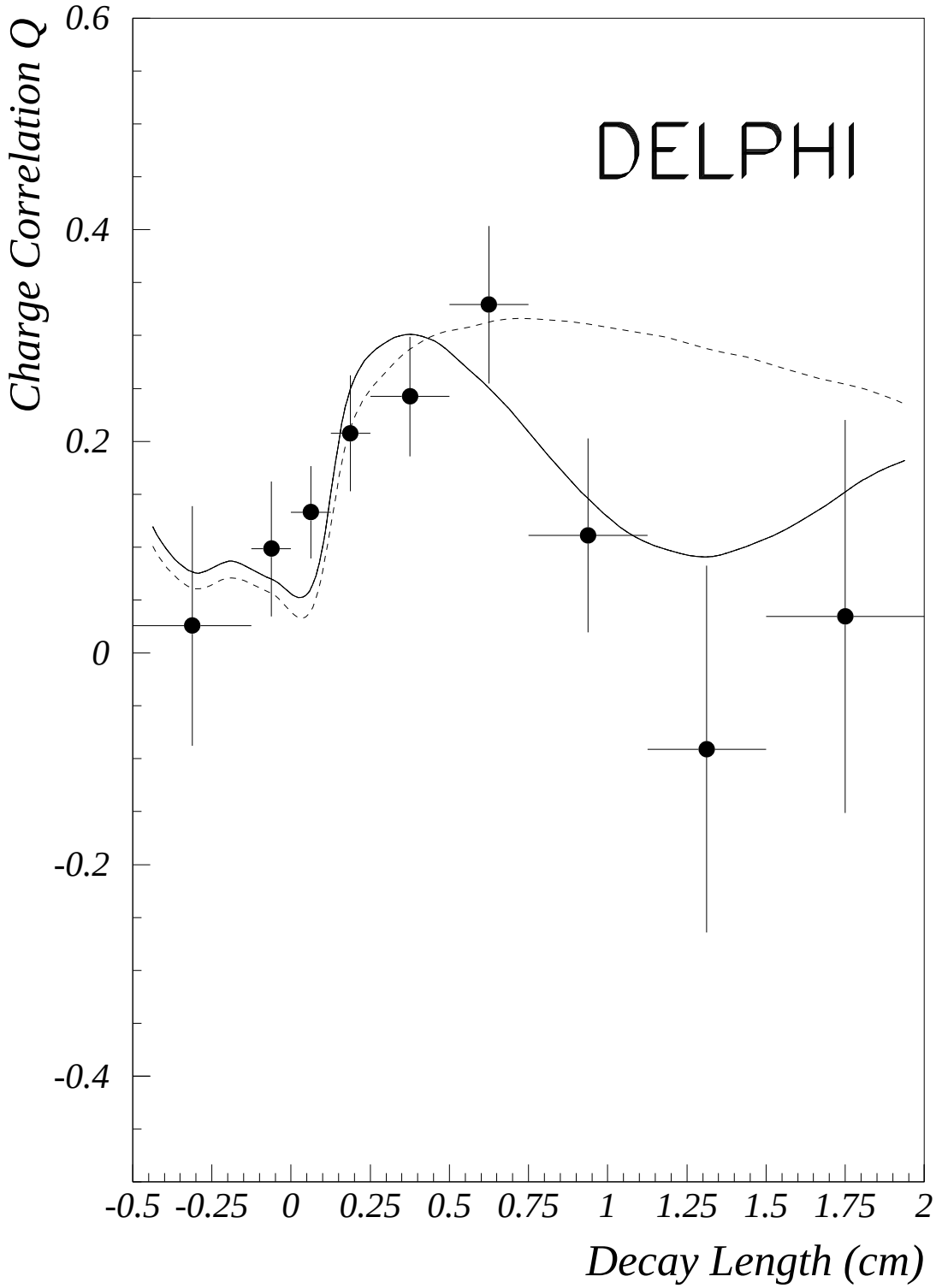

Figure 3: The charge correlation function Q plotted as a function of the D^0 decay length in cm. The full dots with the error bars represent the data. The full curve is the result of the fit corresponding to $\Delta m = 0.50\ \hbar/ps$. The dashed curve corresponds to a time independent mixing hypothesis.

- The fit was repeated using a parametrization of the B^0 momentum as a function of the reconstructed D^* momentum . The fitted value of Δm changed by 1% with respect to the value obtained using a parametrization of the B^0 momentum as a fixed fraction of the beam energy. A further check was performed by using a sample of 30000 generated events, with a simple smearing of the time distribution. The difference between the fitted value of Δm obtained by using the average B momentum and the value obtained by taking the true generated B momentum was found to be negligible.

- The fitting procedure previously described was applied to a generated sample with detailed simulation of the detector, having $\Delta m = 0.475\ \hbar/ps$. The fit was able to reproduce the charge tagging probabilities correctly, and a value of $\Delta m = 0.48 \pm 0.06\ \hbar/ps$ was obtained.

7 Systematic uncertainties

Various possible sources of systematic uncertainty were investigated.

- Time distribution
  Different parametrizations for the time distributions for charm and combinatorial background events were used. The parametrization for the combinatorial background distribution was varied according to the limited data statistics used for its determination. Also, the time resolution σ_t was parametrized as the sum of two Gaussian functions. The observed shifts of the fitted value of Δm were $\pm 0.030\ \hbar/ps$.

- B lifetime
  In addition, for each parametrization, the fitted value of the B lifetime $\tau_B = 1.63 \pm 0.10$ ps was varied by one standard deviation. This produced a change of $\pm 0.010\ \hbar/ps$ on Δm.

- B momentum error
  Changing the B momentum according to the error on the measurement of the average fraction of beam energy $X_B = 0.695 \pm 0.03 \pm 0.01$ [11], Δm varied by $\pm 0.020\ \hbar/ps$. According to the simulation, the mean fraction of beam energy changed by $2 \pm 2\%$ after the D^* selection, and no additional systematic uncertainty was considered.

- $B^{\pm}$ fraction
  Given the limited knowledge of the fraction of $B^{\pm}$ contributing to D^* production, a conservative variation (0.17 ± 0.10) of the expectation was used to estimate a corresponding systematic uncertainty of $\pm 0.025\ \hbar/ps$.

- $r_{c\bar{c}}$ fraction
  The fraction of charm, $r_{c\bar{c}}$, was varied around the value measured from the data $(0.36 \pm 0.05 \pm 0.03)$ by one standard deviation, giving a systematic uncertainty of $\pm 0.020\ \hbar/ps$.

- f_{comb} fraction
  A variation of the fraction of combinatorial background $f_{comb} = 0.318 \pm 0.020$ by

one standard deviation gave a systematic effect of $\pm 0.010\ \hbar/ps$.

- ϵ_{mix}^{unlike}, $\epsilon_{B^{\pm}}^{unlike}$, $\epsilon_{c\bar{c}}^{unlike}$
  The hemisphere charge probabilities depend on the central value and the width of the hemisphere charge distribution, which are taken from the simulation. A possible shift of $\pm 15\%$ of the central value was considered. Also, different values of the weight power factor k between 0.2 and 1.0 were used to estimate the effect of changing the width of the hemisphere charge distribution. The maximum shifts observed in the hemisphere charge probabilities were used to estimate the systematic uncertainties. The probability ϵ_{mix}^{unlike} was changed between 0.504 and 0.565, obtaining $\Delta m = \pm 0.025\ \hbar/ps$. The probability $\epsilon_{B^{\pm}}^{unlike}$ was varied between 0.19 and 0.29 and $\epsilon_{c\bar{c}}^{unlike}$ between 0.56 and 0.64, changing Δm by $\pm 0.005\ \hbar/ps$ and $\pm 0.020\ \hbar/ps$, respectively.

The contributions from the variation of the parameters τ_D and ϵ_{comb}^{unlike} were found to be negligible.

The contribution of the various systematics errors are summarized in Table 2. On summing them in quadrature, an overall systematic error on Δm of $\pm 0.06\ \hbar/ps$ is obtained.

Table 2: Systematic uncertainties. The sign ($\pm$ or $\mp$) shows the correlation with the variation of the relevant parameters.

Contribution	variation on Δm [$\hbar/ps$]
Time distribution parametrization and time resolution	$\pm$ 0.030
B lifetime	$\pm$ 0.010
B momentum parametrization	$\pm$ 0.020
Fraction of $B^{\pm}$	$\mp$ 0.025
Fraction of charm events	$\pm$ 0.020
Fraction of background	$\mp$ 0.010
ϵ_{mix}^{unlike}	$\mp$ 0.025
$\epsilon_{B^{\pm}}^{unlike}$	$\mp$ 0.005
$\epsilon_{c\bar{c}}^{unlike}$	$\pm$ 0.020
Total	$\pm$ 0.06

8 Conclusions

The characteristic time dependence of $B_d^0 - \bar{B}_d{}^0$ oscillations has been observed by using D^*-hemisphere charge correlations. The measured mass difference is:

$$\Delta m = 0.50 \pm 0.12(stat) \pm 0.06(syst)\ \hbar/ps,$$

or, converting into eV/c^2:

$$\Delta m = [3.29 \pm 0.79(stat) \pm 0.39(syst)]\ \ 10^{-4}\ eV/c^2.$$

A model with time independent mixing is disfavored by 2.9 standard deviations.

Assuming that the B_d^0 lifetime is equal to the average B lifetime measured at LEP, $\tau_B = 1.538 \pm 0.033$ ps, the ratio $\Delta m/\Gamma$ is equal to:

$$\frac{\Delta m}{\Gamma} = 0.77 \pm 0.18(stat) \pm 0.09(syst).$$

These results are consistent with the measurements of time dependent B_d^0 mixing performed by the ALEPH [3] and OPAL [4] collaborations.

Acknowledgements

We are greatly indebted to our technical collaborators and to the funding agencies for their support in building and operating the DELPHI detector, and to the members of the CERN-SL Division for the excellent performance of the LEP collider.

References

[1] M. Gell-Mann and A. Pais, Phys. Rev. 97 (1955) 1387

[2] J. Bartel et al. (CLEO Collab.) CLNS/93-1207 (1993),
H. Albrecht et al. (ARGUS Collab.) Z. Phys. C55 (1992)

[3] D. Buskulic et al., (ALEPH Collab.), Phys. Lett. B313 (1993) 498 ;
D. Buskulic et al., (ALEPH Collab.), CERN-PPE/93-221 submitted to Phys. Lett.

[4] R. Akers et al., (OPAL Collab.), contributed paper to Moriond Conference, 1994;
R. Akers et al., (OPAL Collab.), Phys. Lett. B327 (1994) 411;
R. Akers et al., (OPAL Collab.), CERN-PPE/94-90 submitted to Zeit. Phys.

[5] P. Aarnio et al. (DELPHI Collab.), Nucl.Instr. and Meth. A303(1991) 233-276

[6] N. Bingefors et al. (DELPHI Collab.), to be published in Nucl. Instr. and Meth.

[7] P. Abreu et al. (DELPHI Collab.), Phys. Lett. B322 (1994) 459

[8] LUND JETSET 7.3, T. Sjöstrand and M. Bengtsson, Comp. Phys. Comm. 43 (1987) 367

[9] DELPHI Collab., DELSIM DELPHI Event Generation and Detector Simulation User's Guide, DELPHI note 89-67 (1989) unpublished

[10] P. Aarnio et al. (DELPHI Collab.), Phys. Lett. B240 (1990) 271

[11] P. Abreu et al., (DELPHI Collab.), contributed paper at the Marseille Conference, 1993